

Interstellar extinction and the intrinsic spectral distribution of variable carbon stars^{*,**}

A. Knapik and J. Bergeat

Centre de Recherche Astronomique de Lyon (UMR 5574 du CNRS), Observatoire de Lyon, 9 avenue Charles André, F-69561 St-Genis-Laval Cedex, France

Received 15 July 1996 / Accepted 10 October 1996

Abstract. We present a new method of evaluation of the extinction by interstellar dust on cool carbon variables. These late-type stars show no marked relationship between spectral classification (the R, N- and C-types) and photometric colour indices. The pair method is thus ruled out, at least in the form currently in use for early-type or intermediate stars.

Our method makes use of the whole spectral energy distributions from UV to IR. A sample of 60 unreddened carbon variables is delineated and new colour-colour diagrams are proposed where the reddening vector is nearly perpendicular to their narrow intrinsic locus. Six photometric groups (or boxes : CV1 to 6) are derived among unreddened stars. They show a continuous range of spectral energy distributions from “bluer” to “redder”, and mean colour indices are obtained. A pair method is described where each presumably reddened star is compared to these mean unreddened stars, a given extinction law being assumed.

As an illustration, the results are shown for a sample of 133 well-documented stars. The mean extinction law usually adopted for the diffuse interstellar medium ($R_V \approx 3.1$) is shown to provide good fits. The threshold for reddening detection turns to be $E(B - V) \approx 0.02 - 0.03$. A good correlation is observed when the derived colour excesses are compared to values from maps in the literature. The mean rate of visual extinction amounts to $\langle A_V/D \rangle \approx 1.25 \pm 1.1$, ranging from 0.37 near $l \approx 240^\circ$ (intercloud) to 2.1 (cloud + intercloud) in two structures correlated with Gould’s belt.

Key words: stars: AGB and post-AGB – stars: carbon – dust, extinction

Send offprint requests to: J. Bergeat

* This research has made use of the Simbad database operated at CDS, Strasbourg, France.

** Table 3 is only available in electronic form at the CDS via anonymous ftp 130.79.128.5

1. Introduction

The correction for interstellar dust extinction (hereafter extinction) is usually obtained from the comparison of the observed colour indices to the corresponding values for similar unreddened stars (intrinsic colour indices). The matching is obtained from the pair method on the basis of spectral type and luminosity class. This is an approximate approach, specially for luminous red giants in a portion of the H-R diagram where so few parallaxes and absolute magnitudes are available (e.g. Perryman et al. 1995).

The Harvard classification was extended to classical carbon stars by Shane (1928), namely the R and N- types with subdivisions. Keenan & Morgan (1941) gathered them in a single type $C_{i,j}$ with two numbers for subdivisions. Except for the earliest stars (types R or C with first index i in the 0-3 range), this is not a true temperature sequence and reliable luminosity criteria are missing. In addition, no close connexion could be found between photometry and spectral classification. The classical pair method thus cannot be used here. An illustration of what can be done when this is not the case is the work of Lee (1970) on M-type supergiants.

Three different approaches can be found in the literature when extinctions on those stars need to be estimated: an analytical formula based on an assumed continuous spatial distribution of intervening dust with galactic latitude (hereafter called *analytic method*), values derived from other stars in the same field (hereafter *field method*), and the use of colour-colour diagrams such as U-B versus B-V or J-H vs. H-K (hereafter *colours method*). An estimate of the distance is needed in the first two methods. The spatial distribution of extinction may prove quite patchy (e.g. Whittet 1992), and results badly in error may result from the first method. The second one is very often hampered by poor knowledge of true distances. A narrow well-defined intrinsic locus and a reddening vector strongly inclined to it are the main requirements of the colours method. They are not usually fulfilled in the case of carbon stars. For instance, a wide intrinsic locus is observed in the U-B vs. B-V diagram due to the large amplitude of variations in this short wavelength range. This is a rather unfortunate situation since good accuracy would

be expected on the grounds of high extinctions there. The amplitudes of variations are smaller in the near infrared but this is also the case of extinctions, and the angle of the reddening vector to the axis of the intrinsic locus is only about $20 - 30^\circ$ in the J-H vs. H-K diagram (see e. g. Fig. 2 in Claussen et al. 1987). Only large extinctions can thus be obtained. As a part of our method, we show in Sect. 3 a new diagram we found more efficient in the red and near infrared.

We propose a new truly-dedicated method which makes use of the whole spectral energy distribution from ultraviolet to infrared and avoid the above-mentioned drawbacks (Sect. 4). The multicolour photometry used is briefly summarized in Sect. 2 and the intrinsic (unreddened) spectral distributions are derived in Sect. 3. Finally, the results are shown in Sect. 5 for a sample of well- documented semi-regular and irregular variables (SR and L-types respectively in Kholopov et al. 1985, GCVS), hereafter referred to as non-Miras. The small sample of carbon Miras (M-type in GCVS) will be dealt with in a forthcoming paper (Bergeat & Knapik 1996), since specific difficulties arise from their large variations. The carbon stars studied here can usually be found in the General Catalog of Cool Galactic Carbon Stars (Stephenson 1989) which will be referred to as C followed by the star's entry.

2. The selection of multicolour photometry

Ideally, the data would consist in simultaneous photometry secured on the entire spectral range. Sets of nearly simultaneous data are available for a few (usually bright and unreddened) stars (see e.g. Mendoza 1967, or Bouchet 1984 for TW Hor). They are very useful in determining the unreddened spectral distributions but the main data base relies on separate sets like UBVR or JHKL secured at different epochs. Assuming that the variations repeat faithfully, one can look for similar phases when available (date of observations and elements from GCVS). This is not the case for many semi-regular variables, nor of course is it so for irregular ones. Fortunately, their amplitudes of variations are amongst the smallest at a given wavelength, and the consistency of the available photometric sets can frequently be checked. In the following subsections, we briefly introduce the used data and mention a few specific difficulties we faced.

2.1. The short wavelength range

We have collected the UB data available in the references (including catalogs) available at the CDS (Strasbourg). Unfortunately, narrow band photometry and spectrophotometry are available for small samples only and cannot be used in this work. Strong molecular bands (mainly CN and C2) could have been avoided, which significantly affect the UB bands. The UB photometry proves useful due to large extinctions, despite strong molecular absorption and large amplitudes of variations. Clearly the U-filter (with its additional requirement of good blocking of the abundant red radiation from carbon stars) provides less reliable data than the B or V-filter on the average.

2.2. The red and near infrared photometry

Initially, the R ($0.7 \mu\text{m}$) and I ($0.9 \mu\text{m}$) filters from the Arizona photometry (e.g. Mendoza & Johnson 1965) were preferred to the Kron-Cousins R_{KC} ($0.64 \mu\text{m}$) and I_{KC} ($0.8 \mu\text{m}$) filters (e.g. Walker 1979) since the latter bandpass is nearly centered on a strong band head of the red system of CN. Finally, it proved consistent and could be used as well. Most useful here are the simultaneous (or nearly so) UBVR photometry as published in a few references.

We made a large use of the eight-colour narrow band photometry of Baumert (1972) for about 300 carbon stars. We selected his two "continuum points", namely the third filter at $0.78 \mu\text{m}$ and the seventh one at $1.08 \mu\text{m}$ where the above-mentioned CN-bands are minimum. Originally, Baumert's data were not given on a true magnitude system, except those of his fifth filter at $1.04 \mu\text{m}$. We assumed $[1.04] = 0$ for Vega which corresponds to $5.73 \cdot 10^{-13} \text{ W cm}^{-2} \mu\text{m}^{-1}$. Adopting the black body colour temperature and the depressions D as given by Baumert (1972), we deduced fluxes at the continuum points. Then, the $[0.78]$ and $[1.08]$ magnitudes were calculated, with respectively $1.19 \cdot 10^{-12}$ and $5.14 \cdot 10^{-13}$ for the zero-magnitudes fluxes in units of $\text{W cm}^{-2} \mu\text{m}^{-1}$. These numbers were derived by interpolating through the spectral shape of Vega data (Oke & Schild 1970, Schild et al. 1971) and the absolute calibrations of various published photometric systems (Johnson & Mitchell 1975, Bessell 1979). Their accuracy has no influence on our method which is a relative one. The obtained fluxes and magnitudes however proved quite consistent with data from other authors in this range. A precise comparison is nevertheless impossible for these variables with strong molecular bands. Fortunately, two Ba II stars (HR 2392 = NSV 3024 with a small 0.03 mag amplitude in V and HR 8204 not known as a variable) have been observed by Baumert (1972) and Johnson & Mitchell (1975). For both stars, we found that the two flux distributions agree to within $\pm 5\%$ which is satisfactory. We shall write hereafter CI_B for the colour index $[0.78]-[1.08]$.

The used JHKL data was taken from many references which can be found in the third edition of the Catalog of Infrared Observations (Gezari et al. 1993a). Most of them were on the Arizona system or systems close to it. Since data on variable stars were not obtained simultaneously by the various authors, no conversion was attempted between their JHK systems. The largest differences affect probably the J-filter (Bessell & Brett 1988). Concerning the L-filter, we tentatively made the difference between the original band (central wavelength of 3.4 or $3.5 \mu\text{m}$) and more recent implementations (from 3.6 to $3.8 \mu\text{m}$). Hereafter, they are referred to as L and L' respectively. Accordingly, the corresponding magnitudes were treated separately. The differences obtained for many of our variable stars proved however to be small. Simultaneous IJHKL-photometry was quite helpful when available (e.g. Bergeat & Lunel 1980) since the connection to UBVR data is made easier.

As noted by Claussen et al (1987), the photometry by Noguchi et al. (1981) was given on a substantially different system. They used the data of Bergeat & Lunel (1980) to convert

the JHK magnitudes of Noguchi et al. to the Johnson system. Their conversion equations are colour dependent. A strong increase of variability with increasing J-K is observed however, and 23 stars only are found in common. Thus we preferred to simply add 0.36 0.16 and 0.12 mag. to the J, H and K magnitudes (respectively) from Noguchi et al., these values being obtained from a much larger sample. No correction was applied to their L' ($3.7 \mu\text{m}$)-values since the calculated shift amounts to -0.06 ± 0.20 .

2.3. The far infrared photometry

The references may be found in Gezari et al. (1993b). We did not use data secured through M-filters centered between 4.6 and $5.0 \mu\text{m}$. Strong molecular absorption is often present and photometry in this low transmission atmospheric window may be less accurate. Also, we ignored photometry at 8.4 or $8.6 \mu\text{m}$ which is available for a limited sample of carbon stars, mostly unreddened. The IRAS Point Source Catalogue (1988) is the only large data base at hand in the far infrared. We limited our analysis to the first two filters, namely the [12] and [25] magnitudes at $12 \mu\text{m}$ and $25 \mu\text{m}$ respectively. Most of our stars are “optical” carbon stars which frequently show excesses at $60 \mu\text{m}$ attributed to detached circumstellar shells (e.g. Young et al. 1993). Also, at 60 and $100 \mu\text{m}$, the data in the point source catalog may be affected by a residual contamination from cirrus emission, according to the quoted flags. This is expected for reddened carbon stars. We applied the colour correction as described in the IRAS Explanatory Supplement (1988) and convert the fluxes into magnitudes making use of the absolute calibration of Beichman et al. (1990). It should be noted that the [12]-values are influenced by the $11.3 \mu\text{m}$ SiC emission feature when sufficiently strong.

3. A new classification scheme for intrinsic spectral distributions

It is necessary to emphasize here that the used infrared data may be affected by emission from circumstellar dust hotter than its counterpart of the detached shells mentioned in Sect. 2.3.. Some of the stars studied here have in fact been modelled for circumstellar shells of amorphous carbon and SiC grains by Lorenz-Martins & Lefèvre (1994). The derived (extinction) optical depths are typically small, not in excess of 0.2. We made no attempt to subtract such contributions, nor did we correct for corresponding circumstellar extinction. A classification scheme of the intrinsic spectral distributions is established in the present section. These distributions may include circumstellar features. They are used as a reference in our study of extinction from the (presumably diffuse) interstellar clouds on the line of sight to the star.

3.1. A galactic latitude versus colour index diagram

A preliminary work consisted in the determination of the maximum value of a given colour index for our sample of carbon

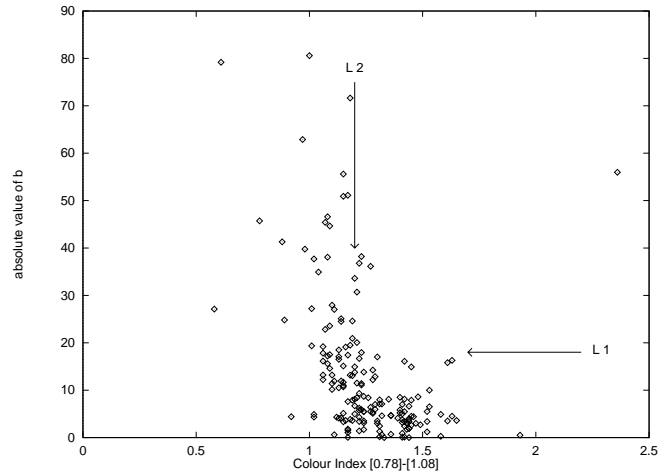


Fig. 1. A diagram of the absolute value of the galactic latitude of carbon non-Miras vs. the CI_B colour index computed from Baumert’s data as described in Sect. 2.2.. The horizontal L1 line delineates the low-latitude high-reddening region while the vertical L2 line corresponds to an estimate of the maximum value of the index for unreddened stars. The star at the extreme right is the infrared carbon star RW LMi = CIT 6.

stars, i.e. the maximum unreddened colour index observed. As an illustration example, we show in Fig. 1 the absolute value of the galactic latitude against the colour index CI_B deduced from Baumert’s data as described in Sect. 2.2. The plot is restricted to the non-Miras studied in the present paper. No clear difference could be found between SR and L-variables in this diagram and the same symbol is subsequently used for both types. A separation line (L1 in Fig. 1) can be drawn which splits the diagram into two parts, namely a strip for $|b| \leq 18^\circ$ where large values of the colour index are observed, and an upper high-latitude region with $CI_B \leq 1.20 \pm 0.03$ (L2 in Fig. 1), except for one star located at the extreme right. This star (RW LMi = CIT6) classified as SRA in the GCVS, is a well-known infrared carbon star with substantial circumstellar extinction and emission, an object similar to IRC +10216. It is not considered any further in this study. The abscissa of L2 is interpreted as the maximum value of the unreddened colour index for carbon non-Miras, and stars below L1 and at the right of L2 are low latitude reddened stars. Close to L2, stars may be reddened, but the reddening should be small, specially above L1. Except for a few stars, the unreddened colour index is restricted to a narrow (1.0-1.2) range which is a remarkable property turned to advantage in Sect. 3.2..

Other colour indices may be used. This is however the diagram of Fig. 1 which proved to be the most accurate one to be available for a large sample of stars. The central wavelengths fall in regions of minimum molecular opacities and the band-passes are narrow. In addition, they are close to wavelengths of maximum flux and photometric accuracy is expected to be good.

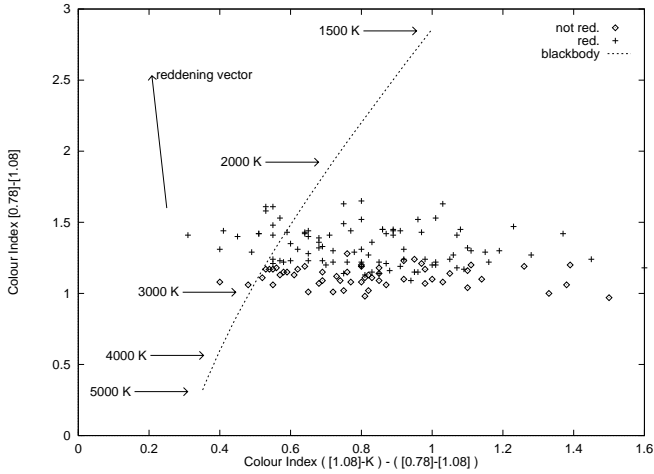


Fig. 2. An optimized colour-colour diagram : the reddening vector of the interstellar extinction is shown to be nearly perpendicular to the horizontal band $CI_B \leq 1.20$ populated by unreddened stars. The blackbody line is also shown for some temperatures.

3.2. An optimized colour-colour diagram

Nearby low-latitude stars of Fig. 1 may well be unreddened and some stars at higher latitudes may be slightly reddened due to the patchy distribution of interstellar dust. Additional information is needed to establish two lists of carbon stars, entitled respectively “certainly reddened” and “possibly unreddened”. We built many colour-colour diagrams following a trial and error method, until we obtain a reddening vector nearly rectangular to a narrow intrinsic locus. These optimized diagrams are finally of the type CI_B plotted against the difference $([1.08]-m_{IR})-CI_B$ where m_{IR} is a magnitude in the near infrared range (H, K, L or L’). Ideally, this magnitude should have been obtained in a third narrow band, the measurements having been simultaneous. No such data is available at present for a large sample of carbon stars and m_{IR} has to be a large band. The J-filter is close to the other filters and a somewhat higher dispersion of the available data is observed. Thus we ignored the corresponding diagram. Finally, the diagram with the K-filter (see Fig. 2) proved to be the best one according to the above-mentioned criterium. These diagrams provide a firm basis to complete a list of reddened stars.

Due to the small (1.0-1.2) range in CI_B , the horizontal width of the intrinsic locus (which amounts to about 1.7 mag.) is mainly due to the range in the $[1.08]-K$ index (as can be seen hereafter in Fig. 3). The index difference $([1.08]-K)-CI_B$ was however adopted in Fig. 2 to obtain a reddening vector nearly rectangular to the intrinsic locus (in the $[0.78]-[1.08]$ vs. $[1.08]-K$ diagram the angle is nearly of 45° only). A similar behavior is observed with the L or L’-magnitudes while a reduced width is obtained with the H-filter. This remarkable result is discussed in Sect. 3.3.. A few variables (not shown in Fig. 2) were found well below the locus of unreddened stars, i.e. in the region populated by the non variable stars of early spectral types (these latter stars cluster around the black body line in the 3000-5000 K range). This is the case for instance of C 327 (V Ari) and C 3319 (TT

CVn) which both are CH stars with large velocities. Together with hotter RCB variables and hydrogen deficient (HdC) stars, they deserve a separate study (Knapik & Bergeat 1996).

3.3. A grid of unreddened spectral energy distributions

In a preliminary approach, we attempted to select couples of carbon stars, the two members being connected in every diagram by a reddening vector. A consistent set of vectors is of course needed to find out the solution. This is just the pair method except for the selection criterium which is a photometric one here. As expected, this method gave seemingly good results for high extinctions. At least, no significant discrepancy from other methods was noted. To increase the accuracy for lower colour excesses, we combined the solutions derived from several unreddened stars located in a photometric box we centered at the origin of the reddening vector. Finally, we prefer to adopt a unique method where the same treatment is applied to every reddened star, whatever the extinction amount may be.

To this purpose, we split our list of unreddened stars into six boxes named CV1 to CV6 (CV is for Carbon Variable). In Fig. 2 and analogs with H, L or L’ instead of K, they spread from left to right through the various locii. The number of boxes was chosen so as to provide regular and significant intervals taking into account the expected accuracies. Here, we must emphasize that no gap is observed which could help. In a way, this process is similar to spectral classification.

Every star selected in these six unreddened samples was carefully screened for possible extinction. In addition to the diagrams like Fig. 1 or 2, the maps of Neckel & Klare (1980) and FitzGerald (1968) were used in a hit-or-miss way. The mean absolute magnitudes $M(104) = -4.7$ at $1.04\mu\text{m}$ (Baumert 1974, 1975) and $M_K = -7.0$ at $2.2\mu\text{m}$ (e.g. Eggen 1972) were used to estimate the stars distances. Both results generally agree within $\pm 10\%$ except for a few stars (specially those with strong infrared excesses). The survey of Burstein & Heiles (1982) from extragalactic sources also provide upper limits of extinction. On this basis, a star was assumed to be “not significantly reddened” and thus selected in a given box, if no evidence of $E(B - V) \geq 0.02 - 0.03$ could be found. As a matter of fact, a few slightly reddened stars escaped detection at this stage. They were evidenced later on from the new pair method described in Sect. 4. We give in Table 1 the number of finally selected stars, and for each box, the GCVS name of a representative star for illustrative purpose. It is worth noting that we could select no more than 60 unreddened stars out of an initial sample of more than 300 stars. The distributions are evolving gradually from the bluer one (CV1) to the reddest one (CV6), a feature illustrated in Table 1 by the $B - V$ mean index on the blue side and the $J - K$ one on the red side.

We finally built the mean spectral energy distributions corresponding to the six boxes. For further use they were calculated as the unreddened value $I_0(\lambda)$ of the colour index $I(\lambda) = m(\lambda) - [1.08]$ where $m(\lambda)$ is the observed (i.e. reddened) magnitude in any filter. They are displayed in Fig. 3 as net fluxes deduced from absolute calibrations. It is remarkable

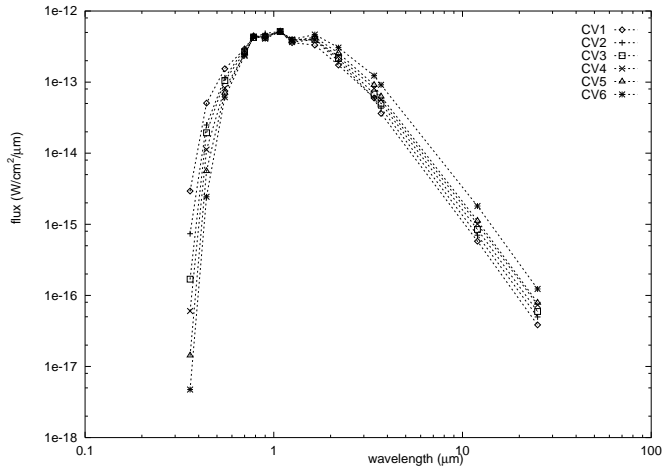


Fig. 3. The absolute spectral energy distributions as derived for the six groups of unreddened variable carbon stars (CV1 to CV6 from the bluest distribution to the reddest one, as quoted in Table 1). Note that the curves are nearly the same in the 0.7 to 1.3 μm spectral range.

Table 1. The six photometric groups (G) of unreddened carbon variables. A representative star is mentioned for each group (name in GCVS) and n is the number of its unreddened members. Three mean color indices are given with their standard deviations (see text for details).

G	TYP.S	n	B-V	CI _B	J-K
CV1	UZ Pyx	8	1.91 ± 0.28	1.06 ± 0.04	1.42 ± 0.07
CV2	NP Pup	11	2.35 ± 0.09	1.12 ± 0.06	1.42 ± 0.07
CV3	U Hya	11	2.47 ± 0.17	1.12 ± 0.05	1.56 ± 0.07
CV4	U Ant	7	2.85 ± 0.12	1.12 ± 0.07	1.71 ± 0.05
CV5	X Cnc	11	3.37 ± 0.16	1.11 ± 0.05	1.75 ± 0.07
CV6	RT Cap	12	4.29 ± 0.29	1.14 ± 0.10	1.95 ± 0.10

that the curves nearly coincide in the red-near infrared part of the spectrum, i.e. in the ranges of the R, I and J-filters from various systems (0.7 to 1.3 μm) and of Baumert's (1972) narrow band photometry (0.71 to 1.1 μm). This is true even in bands where molecular absorption is stronger such as the J-one shown in Fig. 3 or the [0.81] and [1.10]-ones from Baumert which are not shown. His CN-index (red system) thus displays a limited range for carbon variables with no clear correlation with our CV classification.

Early type carbon non-variables and hot variables as mentioned in Sect.3.2. behave differently and a continuous evolution is perceptible for those stars as shown by their CI_B indices for instance. Their CN-index also populates a large range and they closely follow the black body line of Fig. 2 which intersects the locus in the region of the CV1 box. From CV1 to CV6, the fluxes at short wavelengths are increasingly depressed while the infrared radiation strengthens. From blue to infrared, the higher points of the CV1-curve closely match a black body distribution whose temperature lies in the 2800-2900 K range. This

is probably a reasonable estimate of the mean effective temperature of CV1 stars. Lower temperatures (2300-2800 K) are probably the rule for later CV-types (2 to 6). There seems to be more or less strong correlations between our classification and the intensity of various spectral features, either molecular absorption or grain emission. These results will be discussed elsewhere since extinction correction is the main purpose here. Finally, the diagrams which applies in Sect. 3.2. led us to a photometric classification which applies on the whole spectral range from ultraviolet to infrared.

4. The new pair method for carbon stars

4.1. The evaluation of the extinction

Following Mathis (1990), we adopt $\lambda = 1.25 \mu\text{m}$ as a reference wavelength for our extinction study. This is the central wavelength of the J-filter and a large amount of data is available for carbon stars in this band. Actually, this choice is justified by the fact that many lines of sight whose extinction laws differ markedly in the UV and visible, show the same law in the infrared when normalization is secured in the latter range. The departures from the standard mean law of the diffuse medium usually stand out in the 0.7-0.9 μm range. Special laws could presumably be detected from eventual discrepancies between the UBVR-range and the infrared domain. The question of their origin, -that is the diffuse medium, a local cloud or circumstellar shell-, would remain however totally open. The extinction at any wavelength is thus written as the difference between the observed (reddened) and intrinsic (unreddened) magnitudes, namely

$$A(\lambda) = A(J)r(\lambda) = m(\lambda) - m_0(\lambda) \quad (1)$$

where $r(\lambda)$ is the adopted reddening law. Referring to the mean unreddened indices $I_0(\lambda)$ of a given CV-box (see Sect. 3.3.), we calculate for a presumably reddened star the difference

$$y(\lambda) = m(\lambda) - I_0(\lambda) \quad (2)$$

at every observed wavelength. It reduces to $y(\lambda) = [1.08]_0$ when the reddening is found to be negligible : the observed points are then expected to scatter around an horizontal line in Fig. 4. Assuming a given reddening law, this quantity is predicted to amount to

$$y_p(\lambda) = A(J)r(\lambda) + \langle [1.08]_0 \rangle \quad (3)$$

once the extinction $A(J)$ and the unreddened magnitude $\langle [1.08]_0 \rangle$ are known. The latter corresponds to an ideal star whose intrinsic spectral distribution would exactly coincide with the one of a given box (CV1 to CV6). We can see from Eq. (3) that a linear relation of y against r should exist where the slope and intercept are the above-mentioned extinction and unreddened magnitude respectively, provided the right CV-box was selected.

As a starting point, we used the mean law for the diffuse medium as given by Mathis (1990). The plot of y vs. r is shown

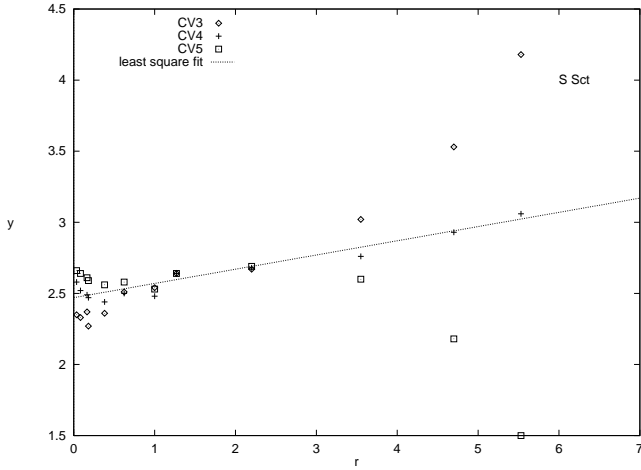


Fig. 4. The plot of the quantity y vs. r illustrating Eq. (2) in the case of C 4121 (S Sct). The abscissae are extinctions normalized at $1.25\mu\text{m}$. The ordinates are the colour excesses plus unreddened magnitude at $1.08\mu\text{m}$ once a linear fit is obtained for a given box (here CV4). The intercept is thus $[1.08]_0$ since the colour excess vanishes with extinction. The straight line was derived from the least square method (see text for details). Its slope is an evaluation of the extinction at $1.25\mu\text{m}$, namely 0.10 ± 0.01 (internal error).

in Fig. 4 for the star C 4121 (S Sct) as an illustration. A good linear relation is obtained if the CV4 group is adopted while distorted curves are observed when the indices of the nearest boxes (CV3 and CV5) are used. As precedently noted, peculiar reddening laws are usually expected in the short wavelength range (UBVR) only. On the contrary, the curvatures observed in Fig. 4 with CV3 or CV5 are spread on the whole spectral range. We conclude that they are a consequence of photometric box mismatch and we feel confident that the good fit obtained with CV4 is not fortuitous. We were able to reach such a solution for any well-documented carbon non-Mira studied so far (see however the restrictions mentioned in Sect. 4.2.).

The extinction derived for C 4121 is $A(J) = 0.10 \pm 0.01$ where 0.01 mag is the standard deviation of the slope σ_a as given by

$$\sigma_a^2 = \frac{\sum (y - y_p)^2}{(n - 2) \sum (r - \langle r \rangle)^2} \quad (4)$$

where $\langle r \rangle = (\sum r)/n$. This is an estimate of the internal accuracy achieved on our extinction evaluation. We may deduce the usual colour excess which is for the diffuse law

$$E(B - V) = A(J) / 0.873 \quad (5)$$

For C 4121 it amounts to nearly 0.12 mag to compare to 0.14 mag as read from the map (zone 258) of Neckel & Klare (1980) if a 300-340 pc distance is adopted.

The quality of the linear fit may also be estimated by making use of the correlation coefficient

$$\rho = \frac{(ry - n \langle r \rangle \langle y \rangle)}{(\sum r^2 - n \langle r \rangle^2)^{1/2} (\sum y^2 - n \langle y \rangle^2)^{1/2}} \quad (6)$$

which lies in the 0-1 range. It amounts to 0.98 for C 4131 which is a high value for such a small slope (0.10). Even larger values are usually obtained for larger extinctions, frequently ranging from 0.99 to 1. We also checked the stars in the unreddened list against the mean spectral distribution of their (CV1 to CV6) group. As expected, very low correlation coefficients were obtained except for a few stars whose slight reddenings were thus detected. Finally, 60 stars remain in our list of unreddened stars (see Table 2).

4.2. A study of the residues

The differences $Y(\lambda) = y(\lambda) - y_p(\lambda)$ were systematically analyzed for possible residual dependence on wavelength. To this purpose, the above least square analysis is applied to Y , and the new slope and determination coefficient should be as close to zero as possible. Strong discrepancy of a given measurement may lead to reject it and start again the analysis of Sect. 4.1.. Consistent discrepancies on a large wavelength interval did alert us about group mismatch or even absence of relevant group. The latter case was observed for a few SC or CS stars whose predominant opacities might differ from those of pure C-type stars. They are not studied here. We thought that departures from the standard extinction for the diffuse medium could also be detected. Most observed UBV discrepancies correspond to measurements secured close to variables minimas. We tentatively assume that the reference distributions of Sect. 3.3. are, in this range, essentially valid at maximum light or at an intermediate level. This fact was further checked on a few well-documented stars including TW Hor we mentioned at the beginning of Sect. 2. On the contrary, reliable UBV data was sometimes missing and the corresponding star had to be rejected except if sufficient confidence was obtained from data at longer wavelengths.

Occasionally, we observed a noticeable curvature in the near infrared even larger in the IRAS range, while a reasonable fit was obtained at shorter wavelengths. This behavior is typical of many carbon Miras, and infrared carbon stars (not studied here). It is usually attributed to emitting dust with large optical depth. Part of the IRAS carbon stars are still more extreme in this respect. These objects deserve a separate study (Bergeat & Knapik 1996). Finally, we present the results for 133 well-documented reddened carbon variables in Table 3.

4.3. The proportionality factors of dereddened spectral distributions

The dereddening is finally obtained from Eq. (1). Ideally, we would have

$$m_0(\lambda) - I_0(\lambda) = \langle [1.08]_0 \rangle = -2.5 \log(k) \quad (7)$$

at every wavelength but some scatter is of course observed. Thus we calculate the mean value $\langle k \rangle = \sum k(\lambda) / n$ whose standard deviation is given by

$$\sigma_k^2 = \frac{\sum (k - \langle k \rangle)^2}{n - 1} \quad (8)$$

It may be used as a signal to noise ratio for the whole method.

Table 2. A list of the sixty unreddened carbon variables found in the present study. The stars entries in the C-catalogue (Stephenson 1989) are given. By “unreddened”, we mean a star with $E(B - V) \leq 0.02 - 0.03$ (see Subsec. 3.3. for details).

CV1	CV2	CV3	CV4	CV5	CV6
32	471	234	769	65	36
1004	788	1355	1316	853	1052
1507	1264	1489	2641	2077:	1057:
1737	1478	1565	2685	2177	1877
2331	1881	1653	2793	2378	2150
2635	2713	1944	3368	3283	2384
3227	2835	2244	4302	3313	2738
3558	3665	2803		3481	2877
	3731	3374		3510	3236
	5228	5418		3569	3861
	5928	5987		4307	4774
					5425

The k-coefficient of Eq. (7) is the ratio of the dereddened star fluxes to those of a reference star of the same group (CV1 to 6) which would have the magnitude zero at $1.08\mu\text{m}$. The same ratio should nearly prevail for integrated fluxes since the spectral regions of significant contribution were all covered. Regions of strong molecular absorptions were avoided and differences there may have remained undetected. Of course, the same ratio can directly be computed for unreddened stars. Assuming every star in a given group to be an only star placed at different distances from sun, the k-factor would then be the inverse squared ratio of their distances to the sun. The validity of this assumption is not warranted at all by the data at hand. A substantial range in luminosity and radius may well exist for a given effective temperature, and astrometric data from HIPPARCOS will probably shed some light on that question.

5. The results

5.1. Unreddened carbon variables

As mentioned in Sect. 3, we were unable to find more than 60 unreddened stars out of a sample of at least 300 cool carbon variables. They are listed in Table 2. The reader is referred to Sects. 3 & 4 for details of our analysis. Here, we only recall the meaning of “unreddened” that is “not significantly reddened” to the accuracy of the present method. The upper limit is usually $E(B - V) \approx 0.02 - 0.03$. We also recall that the Mira variables and the hot RCB variables are not included here. Cool carbon variables are distant, intrinsically bright objects. The stars of the unreddened sample are either located in the local dust void of 200-300 pc radius or more distant objects seen at high latitudes and/or through transparent windows.

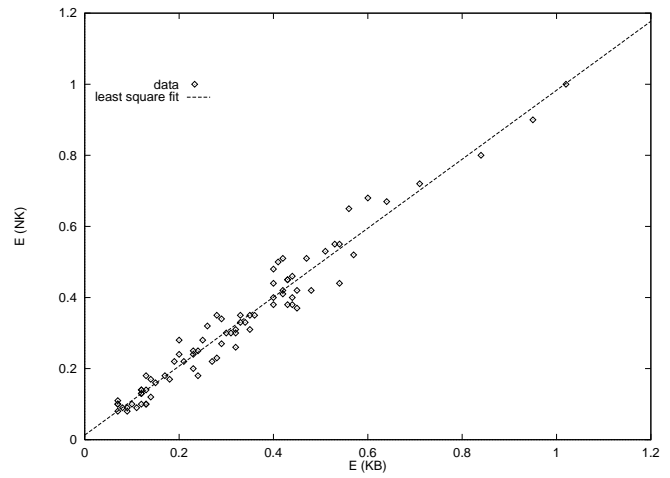


Fig. 5. A comparison of $E(B - V)$ excesses from the maps and graphs of Neckel & Klare (1980) with values from the present paper (E_{KB}). The regression line (9) is also shown.

5.2. A comparison of obtained extinctions to values from the field method

No comparison is attempted with extinction values from the analytic method or colours method (see Sec. 1 for definitions). Instead we concentrate on data derived from other (hot O, B and A) stars in the same fields. We expect good agreement in the zones where extinction is uniform enough, but marked discrepancies should also be observed where patchiness is the rule. To validate our method, we have compared our $E(B - V)$ values from Table 3 to those obtained from published maps and graphs vs. distance (see Sect. 3.3.).

The $E(B - V)$ excesses from the maps and graphs of Neckel & Klare (1980) are shown in Fig. 5 against our values. The plot is limited to their zones where a reasonably unambiguous estimate can be obtained. Discrepant stars are not shown. When only one star in one zone is affected or if several stars in a same zone show various discrepancies, it is impossible to conclude that either method is wrong since patchiness may explain. On the contrary, marked discrepancies can be confirmed from several stars : this is the case in Zone 300 of Neckel & Klare where their plot yields $E(B - V) \leq 0.9$ while we derive about 1.6 from 3 stars in 3 distinct CV-boxes. Finally, we obtain for data of Fig. 5 the linear fit :

$$E_{NK} = 0.970 E_{KB} + 0.013 \quad (9)$$

with a correlation coefficient of 0.979 (see Eq. 6 for a definition). The standard deviation on the slope is 0.023 while it is 0.04 on a single ordinate estimate. The first bisector is thus within the error domain in this diagram.

The comparison with the data of FitzGerald (1968) is more difficult. Its colour excesses are mapped by 0.1, 0.2 or 0.3 mag intervals at four reference distances (0.5, 1, 1.5 et 2 kpc). The corresponding plot (not shown here) is thus very wide, but show no systematic discrepancy between both studies. The detailed

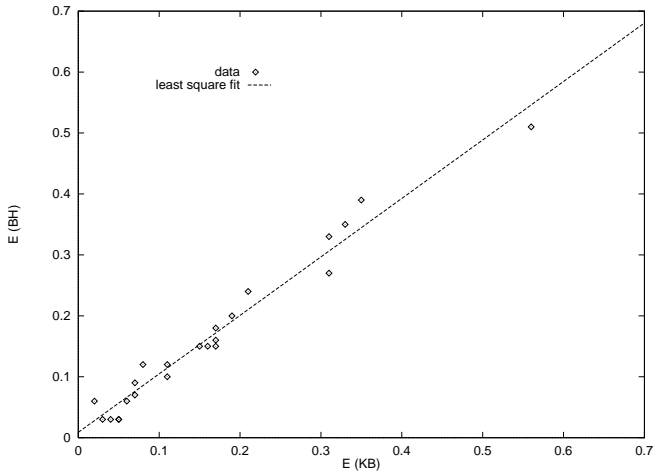


Fig. 6. For stars distant from the galactic plane (see text), a comparison of $E(B - V)$ excesses as taken from the maps of Burstein & Heiles (1982) to our values. The regression line (10) is also shown.

maps of Burstein & Heiles (1982) provide an upper limit to obscuration along a given line of sight. We have considered their value as a reasonable estimate when the distance to the galactic plane ($D |\sin b|$) amounts at least to 100-150 pc. The excesses estimated from their contours are plotted in Fig. 6 against our data. The comparison is unfortunately limited to 23 stars since high latitude cool carbon variables are usually nearby objects with little (or no) reddening. For Fig. 6 data, the linear fit is :

$$E_{BH} = 0.960 E_{KB} + 0.009 \quad (10)$$

with a correlation coefficient of 0.983 (see Eq. 6 for a definition). The standard deviation on the slope is 0.039, while 0.024 is found for a single ordinate estimate. Here also the first bissector falls within the error domain of the diagram.

The slopes (and intercepts as well) are close to each other in Eqs. (9) & (10), and they lead to a mean value of 0.965, i.e. 3.5% lower than expected. This might be a coincidence since they both lie in the error domain, or a systematic effect. It is necessary to recall here that our method yields $A(J)$ which is used to deduce $E(B - V)$ from Eq. (5) whose 0.873 coefficient was adapted from Mathis (1990). Savage & Mathis (1979) already gave 0.87. This number is however dependent on the ratio $R_V = A_V/E(B - V) = 3.1$ adopted by these authors. Slightly different value are often quoted (e.g. 3.05 by Whittet 1992). These comparisons show that our method is valid and that no systematic discrepancy is observed.

5.3. The galactic distribution of reddening material

The distances estimated as described in Sec. 3.3. range from 300 pc to 2.5 kpc, with a strong concentration in the 600-1600 pc interval. Our data carries practically no information on the distribution of the reddening material with galactic latitude since the carbon variables are rather concentrated towards the galactic plane (see for instance the mean values as quoted in the third

Table 4. The distribution with galactic longitude of the mean rate of visual extinction on the line of sight to 133 carbon variables (see text for details). Also given the number n of stars studied per zone and their mean absolute galactic latitude.

l-range	n	$\langle b \rangle$	$\langle A_V/D \rangle$
330-10	11	5.2 ± 2.5	2.14 ± 0.95
10-50	15	5.8 ± 5.2	2.20 ± 1.62
50-90	14	5.7 ± 4.1	1.23 ± 1.10
90-110	8	9.5 ± 7.9	0.78 ± 0.36
110-150	9	5.6 ± 6.0	2.21 ± 1.31
150-190	16	3.4 ± 4.8	1.50 ± 0.84
190-210	9	7.0 ± 8.3	0.90 ± 0.56
210-230	10	5.5 ± 4.6	0.71 ± 0.51
230-250	10	5.7 ± 4.6	0.37 ± 0.23
250-290	14	6.4 ± 4.4	0.63 ± 0.42
290-330	16	10.5 ± 12.0	0.90 ± 0.50

column of Table 4). From our 133 best-studied reddened stars, the mean rate of visual extinction with respect to distance is :

$$\langle A_V/D \rangle = 1.25 \pm 1.08 \quad (11)$$

As evident from Table 4, the large standard deviation on this mean is mainly due to variations with galactic longitude. They correspond fairly well with a local dust distribution partly associated with Gould's belt (see e.g. Fig. 1.3 of Whittet 1992, p. 9) : a structure of thick clouds in the range $l = 330$ to 50° (essentially above the galactic plane) and in the range 100 to 190° (one symmetric about plane between 100 and 130° and the other below plane beyond 150°). A clear region is observed in the range 220 to 270° where our mean rate falls down close to the value of 0.3 mag/kpc as quoted by Allen (1973) for grains between clouds. From Table 4, the maximum mean rate reaches about 2.1 which is close to the 1.9 mag/kpc given by Allen for total (clouds + intercloud) extinction. A slightly lower value of 1.8 is given by Whittet (1992, p. 11).

6. Conclusion

We have delineated a sample of 60 unreddened carbon variables (see Table 2) and classified them into six groups (or boxes : CV1 to 6) according to their whole spectral energy distribution from UV to ir. This has been obtained by introducing new colour-colour diagrams with reddening vector nearly perpendicular to a narrow intrinsic locus (see e.g. Fig. 2) and galactic latitude vs colour index diagrams (Fig. 1). The reference distributions refer essentially to stars at maximum or intermediate light, large amplitude variables at minimum light being not considered here. The curves coincide roughly in the red-near infrared part (0.7 to $1.3 \mu\text{m}$) of the spectrum. This remarkable property occurs in the spectral region of maximum in the corresponding black body radiation. It is probably fortuitous as a consequence of increasing opacities with decreasing temperatures in a limited range (2900-2300 K). Correlations of our CV-classification with

spectral features are currently investigated. For instance the intensity of the $11\mu\text{m}$ emission band attributed to SiC increases from none at CV1 to maximum at CV6.

Then, a new method of extinction evaluation has been described which relies on the whole spectral distribution : this is a generalized colours method and also a pair method with six mean reference stars. The mean extinction law of the diffuse interstellar medium ($R_V \approx 3.1$; e.g. Mathis 1990) is shown to hold good. The near infrared extinction $A(J)$ at $1.25\mu\text{m}$ and unreddened $[1.08]_0$ are determined through a least square analysis of a linear fit (see for ex. Fig. 4). As a by-product, every reddened or unreddened star classified in a CV-group is given a k-scale factor (cf Eq. 7) which should be an angular diameter on a relative scale. A comparison to measurements from occultations and interferometry will be interesting if enough data can be collected. Extinction on the line of sight to 133 well-documented reddened variables is given in Table 3. Extensions of the present work to Miras and hot carbon stars are currently near completion.

Finally we have compared the obtained colour excesses $E(B - V)$ to the values from the field method, i.e. published for zones delimited on the sky. A good agreement is obtained for many well-documented stars (see Figs. 5 & 6). Linear fits are derived for two samples of 80 and 23 stars in common respectively. A mean rate of visual extinction of $(1.25 \pm 1.08)\text{mag/kpc}$ is deduced from a sample of 133 stars. Its distribution with galactic longitude ranges from 0.37 to 2.1-2.2, i.e. from an intercloud rate through a "transparent" window to a cloud + intercloud one elsewhere.

We are currently extending our sample of reddened carbon stars studied. Provided sufficient photometric data is obtained, more distant and highly-reddened objects could be investigated and a probing of the galactic disk then achieved. Ideally, new simultaneous narrow band photometry avoiding the strong molecular band heads would be much helpful. It should be distributed so as to populate efficiently the diagrams such as our Fig. 4.

References

- Allen, C.W., *Astrophysical Quantities*, 1973, The Athlone Press, p. 263
 Baumert, J.H., 1972, The Ohio State university : unpublished thesis
 Baumert, J.H., 1974, *ApJ* 190, 85
 Baumert, J.H., 1975, *ApJ* 200, L141
 Beichman, C.A., Chester, T., Gillett, F.C., et al., 1990, *AJ* 99, 1569
 Bergeat, J., Knapik, A., 1996 in preparation
 Bergeat, J., Lunel, M., 1980, *A&A* 87, 139
 Bessell, M.S., 1979, *Dudley Obs. Repr.* 14, 279
 Bessell, M.S., Brett, J.M., 1988, *PASP* 100, 1134
 Bouchet, P., 1984, *A&A* 139, 344
 Burstein, D., Heiles, C., 1982, *AJ* 87, 1165
 Claussen, M.J., Kleinman, S.G., Joyce, R.R., Jura, M., 1987, *ApJS* 65, 385
 Eggen, O.J., 1992, *AJ* 104, 275
 FitzGerald, M.P., 1968, *AJ* 73, 983
 Gezari, D.Y., Schmitz, M., Pitz, P.S., Mead, J.M., 1993a, NASA Reference Publication 1294, *Catalog of Infrared Observations*, Third Edition
 Gezari, D.Y., Schmitz, M., Pitz, P.S., Mead, J.M., 1993b, NASA Reference Publication 1295, *Far Infrared Supplement*, Third Edition
 IRAS Explanatory Supplement, version 2 1988, Joint IRAS Science Working Group, IRAS Catalogs & Atlases vol. 1, NASA RP-1190, Washington, DC : U.S. Government Printing Office
 IRAS Point Source Catalog, version 2 1988, Joint IRAS Science Working Group, vol. 2-6, NASA RP-1190, Washington, DC : U.S. Government Printing Office
 Johnson, H.L., Mitchell, R.I., 1975, *Rev. Mexic. Astr. y Astroph.* 1, 299
 Keenan, P.C., Morgan, W.W., 1941, *ApJ* 94, 501
 Kholopov, P.N., Samus, N.N., Frolov, M.S., et al., 1985 *General Catalogue of Variable Stars = GCVS*. Nauka Publishing House, Moscow
 Knapik, A., Bergeat, J., 1996 in preparation
 Lee, T.A., 1970, *ApJ* 162, 217
 Lorenz-Martins, S., Lefèvre, J., 1994, *A&A* 291, 831
 Mathis, J.S., *ARA & A* 28, 37
 Mendoza, E.E., 1967, *Tonantzintla and Tacubaya Obs. Bull.* 28, 114
 Mendoza, E.E., Johnson, H.L., 1965, *ApJ* 141, 161
 Neckel, T., Klare, G., 1980, *A&AS* 42, 251
 Oke, J.B., Schild, R.E., 1970, *APJ* 161, 1015
 Perryman, M.A.C., Lindegren, L., Kovalevsky, J., et al., 1995, *A&A*, 304, 69
 Savage, B.D., Mathis, J.S., 1979, *ARA & A* 17, 73
 Schild, R.E., Peterson, D.M., Oke, J.B., 1971, *APJ* 166, 95
 Shane, C.D., 1928, *Lick Obs. Bull.*, 13, 123
 Stephenson, C.B., 1989, *Pub. of the Warner & Swasey Obs.* 3, No. 2
 Walker, A.R., 1979, *South Afric. Astron. Circ.* 1, 112
 Whittet, D.C.B., 1992, *Dust in the Galactic Environment*. Institute of Physics Publishing, Bristol & New York, Ch. 1
 Young, K., Philips, T.G., Knapp, G.R., 1993, *ApJ* 409, 725